

**GEOPHYSICAL PARAMETERS FOR
SEDIMENTARY ROCK IN NORTHWESTERN
PENINSULA MALAYSIA**

HAZRUL HISHAM BIN BADRUL HISHAM

UNIVERSITI SAINS MALAYSIA

2017

**GEOPHYSICAL PARAMETERS FOR
SEDIMENTARY ROCK IN NORTHWESTERN
PENINSULA MALAYSIA**

by

HAZRUL HISHAM BIN BADRUL HISHAM

**Thesis submitted in fulfillment of the
requirements for the degree of
Master of Science**

JULY 2017

ACKNOWLEDGEMENT

I would like to express my deepest gratitude to my supervisor, Dr. Nordiana Mohd. Muztaza for guiding me from the first day till the very end of this research studies. I would also like to give unlimited thanks to my co-supervisor, Dr. Teoh Ying Jia for being very helpful in the geology part of this research. My sincere thank goes to the lecturers of Geophysics Section, School of Physics for being friendly and concern throughout the year. My grateful thanks to the technical staff of Geophysics Section, School of Physics for the assistance and commitments – Mr. Azmi Abdullah, Mr. Yaakub Othman and Mr. Abdul Jamil Yusuf.

During data acquisition, I am indebted to many of my colleague, Mohammad Noor Akmal Anuar, Muhamad Afiq Saharudin, Muhamad Taquiuddin Zakaria, Nabila Sulaiman, Nordiana Ahmad Nawawi, Umi Maslinda Anuar and Nur Amalina Mohd. Khoirul Anuar for being very helpful at the site, also throughout the research writing. Special thanks also go to other postgraduate students who have helped me either directly or indirectly during my studies.

My deepest gratitude goes to the Ministry of Higher Education (MoHE) for sponsoring my tuition fees (MyMaster) under the MYBRAIN15 programme.

It would not have been possible to complete my studies without the help from my parents, their consistent encouragement for me to pursue this level of education since the very beginning is very much appreciated. Finally, Alhamdulillah.

TABLE OF CONTENTS

Acknowledgement	ii
Table of Contents	iii
List of Tables	vii
List of Figures	viii
List of Symbols	xii
List of Abbreviations	xiv
Abstrak	xv
Abstract	xvii

CHAPTER 1 INTRODUCTION

1.0	Background	1
1.1	Sedimentary rock	1
1.2	Problem statement	2
1.3	Research objectives	3
1.4	Scope of the study	3
1.5	Novelty of the study	4
1.6	Thesis layout	5

CHAPTER 2 LITERATURE REVIEW

2.0	Introduction	7
2.1	Seismic refraction tomography theory	7
2.2	Electrical resistivity tomography theory	11
2.3	Porosity and permeability	15
	2.3.1 Porosity	15
	2.3.2 Intrinsic permeability	16
	2.3.3 Klinkenberg effect	17

2.4	Previous study	18
2.4.1	Integration of geophysical and geotechnical survey	18
2.4.2	Geophysical survey	24
2.4.3	Geological study	27
2.4.4	Petrophysical study	29
2.5	Summary	31
CHAPTER 3 METHODOLOGY AND MATERIALS		
3.0	Introduction	33
3.1	Geological of Northwestern Peninsula Malaysia	34
3.1.1	Semanggol Formation	35
3.1.2	Chepor Member	36
3.1.3	Kubang Pasu Formation	37
3.2	General geology of study area	38
3.2.1	Locality 1: Bukit Kukus, Kuala Ketil, Kedah	39
3.2.2	Locality 2: Kulim – Baling, Kedah	41
3.2.3	Locality 3: Bumita Quarry, Utan Aji, Perlis	42
3.2.4	Locality 4: Sanai Hill B, Guar Jentik, Perlis	44
3.2.5	Locality 5: Bukit Chondong, Beseri, Perlis	46
3.3	Data acquisition	48
3.4	Data processing	48
3.4.1	Seismic refraction tomography	49
3.4.2	Electrical resistivity tomography	50
3.5	Porosity and permeability test	51
3.5.1	Water immersion under vacuum	52
3.5.2	Gas permeability measurement	53
3.6	Summary	55

CHAPTER 4 RESULTS AND DISCUSSIONS

4.0	Introduction	57
4.1	Results and discussions	57
4.2	Semanggol Formation	58
4.2.1	Permian facies at Bukit Kukus	58
4.2.1(a)	Geophysical results	60
4.2.1(b)	Rock and petrologic properties	64
4.2.2	Triassic facies in Kulim – Baling area	67
4.2.2(a)	Geophysical results	68
4.2.3	Difference of Permian and Triassic facies	70
4.3	Chepor Member of Kubang Pasu Formation	71
4.3.1	Bumita Quarry, Utan Aji	71
4.3.1(a)	Geophysical results	72
4.3.2	Hill B, Guar Jentik	76
4.3.2(a)	Geophysical results	76
4.3.3	Rock and petrologic properties of Chepor Member	80
4.3.4	Integration of Chepor Member parameters	82
4.4	Uppermost Kubang Pasu Formation	82
4.4.1	Geophysical results	83
4.4.2	Rock and petrologic properties	85
4.5	Comparison of geophysical results with theory value	88
4.6	Summary	91

CHAPTER 5 CONCLUSION AND RECOMMENDATIONS

5.0	Conclusion	93
5.1	Recommendations	95

REFERENCES	96
-------------------	-----------

APPENDIX
LIST OF PUBLICATIONS

LIST OF TABLES

		Page
Table 1.1	Groups of sedimentary rock (Tucker, 1981).	2
Table 2.1	Seismic velocity table of sedimentary rock (Reynolds, 1997).	11
Table 2.2	Resistivity table of sedimentary rock (Loke, 1999).	14
Table 2.3	Physical properties of calcarenite rocks.	22
Table 4.1	Parameters table of chert and claystone of Permian facies at Bukit Kukus.	66
Table 4.2	Table of geophysical parameters with Triassic facies of Tawar chert.	69
Table 4.3	The difference of Permian and Triassic chert.	71
Table 4.4	Table of geophysical parameters with Chepor Member at Utan Aji.	76
Table 4.5	Table of red mudstone and sandstone facies at Hill B, Guar Jentik with geophysical parameters.	78
Table 4.6	Parameters table of CM.	82
Table 4.7	Parameters table of KPF.	87
Table 4.8	Table of geophysical parameters with rock properties.	92

LIST OF FIGURES

		Page
Figure 2.1	Ray paths for seismic waves.	8
Figure 2.2	Compressional and dilation due to ground particle motions.	9
Figure 2.3	Diagrammatic of SRT (Modified from Redpath, 1973).	10
Figure 2.4	Electrical resistivity with relation of resistance (R), area (A) and length (l).	12
Figure 2.5	Four electrode array to measure the subsurface resistivity (Loke, 1999).	13
Figure 2.6	Current is induced between paired electrodes (red lines). Potential difference between paired voltmeter electrodes is measured (after Anderson and Croxton, 2008).	14
Figure 2.7	Seismic section at Ulu Tiram, Johor (Edy et al., 2015).	19
Figure 2.8	Relationship between soil electrical resistivity with water content for all data (Ozcep et al., 2009).	20
Figure 2.9	Correlation between measured water content and inverted resistivity (Cosenza et al., 2006).	21
Figure 2.10	Interpretation of a faulted sequence in Staffordshire. (a) 2-D model. (b) Computed apparent resistivity pseudosection. (c) Field data. (d) Geological interpretation based on (a) and additional information (Griffiths and Barker, 1992).	25
Figure 2.11	Seismic section of three lines at Kaki Bukit, Perlis (Ismail et al., 2013).	26
Figure 2.12	ERT at limestone area in Beseri, Perlis (Muztaza et al., 2013).	27
Figure 2.13	Sedimentological log of the outcrop at Bintulu New Airport (Teoh and Rahman, 2009).	31
Figure 3.1	Flow chart of methodological research.	34

Figure 3.2	Geology map of Semanggol Formation (Basir and Zaiton, 2007).	36
Figure 3.3	Geological map at (a) Utan Aji and (b) Sanai Hill B, Guar Jentik (Meor, 2013).	37
Figure 3.4	Geological map of Bukit Chondong (Meor, 2013).	38
Figure 3.5	Map of study area.	39
Figure 3.6	Study area at Bukit Kukus, Kedah (Google Earth, 2016).	40
Figure 3.7	Bukit Kukus outcrop.	41
Figure 3.8	Study area at Kulim – Baling area (Google Earth, 2016).	42
Figure 3.9	Tawar chert outcrop in Kulim – Baling.	42
Figure 3.10	Study area at Utan Aji, Perlis (Google Earth, 2016).	43
Figure 3.11	Utan Aji outcrop.	44
Figure 3.12	Study area at Guar Jentik, Perlis (Google Earth, 2016).	45
Figure 3.13	Sanai Hill B, Guar Jentik outcrop.	45
Figure 3.14	Study area at Bukit Chondong (Google earth, 2016).	46
Figure 3.15	(a) Depositional model for the coarsening upward facies successions in the uppermost Kubang Pasu Formation (Meor, 2013) and (b) Bukit Chondong outcrop.	47
Figure 3.16	Seismic traces of 24 geophones.	49
Figure 3.17	Travel time curve produced from first arrival picking.	50
Figure 3.18	Flow chart of seismic refraction data processing.	50
Figure 3.19	Cutting the rock samples into cylindrical shape.	52
Figure 3.20	Equipment for porosity test.	53
Figure 3.21	Gas permeability apparatus.	55
Figure 3.22	(a) Metal casing contained rock specimen and (b) flow meter.	55
Figure 4.1	Bukit Kukus outcrop.	59
Figure 4.2	Seismic refraction tomography at Bukit Kukus, Kedah.	60

Figure 4.3	Overlaying SRT result on the outcrop at Bukit Kukus.	61
Figure 4.4	Inversion model of 2-D resistivity of (a) Pole – dipole array and (b) Wenner – Schlumberger array at Bukit Kukus, Kedah.	62
Figure 4.5	Overlaying ERT inversion model on the (a) outcrop, (b) Pole – dipole array and (c) Wenner – Schlumberger array at Bukit Kukus outcrop.	63
Figure 4.6	Comparison of (a) seismic velocity with inversion model resistivity of (b) Pole – dipole and (c) Wenner – Schlumberger array at Bukit Kukus.	64
Figure 4.7	Rock sample of (a) laminated claystone and (b) chert.	64
Figure 4.8	Thin section photomicrographs of chert by (a) cross-polarized light and (b) plane-polarized light.	65
Figure 4.9	Outcrop of Tawar chert. Small picture shows the thinly bedded chert.	67
Figure 4.10	Seismic refraction tomography at Tawar chert outcrop.	68
Figure 4.11	2-D resistivity inversion model of Wenner – Schlumberger array of Tawar chert in Baling area.	69
Figure 4.12	Geophysical tomography superimposed on the outcrop.	70
Figure 4.13	Geological outcrop at Bumita Quarry, Utan Aji.	72
Figure 4.14	Seismic refraction tomography at Bumita Quarry, Utan Aji.	73
Figure 4.15	Inversion model of 2-D resistivity of (a) Pole – dipole array and (b) Wenner – Schlumberger array at Bumita Quarry, Utan Aji.	74
Figure 4.16	Comparison of seismic velocity and inversion model of 2-D resistivity at Bumita Quarry, Utan Aji.	75
Figure 4.17	Outcrop at Hill B, Guar Jentik.	76
Figure 4.18	Seismic refraction tomography at Hill B, Guar Jentik.	77
Figure 4.19	Inversion model resistivity of (a) Pole – dipole array and (b) Wenner – Schlumberger array at Hill B, Guar Jentik.	78

Figure 4.20	Overlaying ERT inversion model on the (a) outcrop, (b) Pole – dipole array and (c) Wenner – Schlumberger array at Hill B, Guar Jentik.	79
Figure 4.21	Rock sample of (a) red mudstone and (b) grey mudstone of Chepor Member.	80
Figure 4.22	Thin section photomicrographs of (a) red mudstone and (b) grey mudstone of Chepor Member.	81
Figure 4.23	Outcrop at Bukit Chondong, Beseri.	83
Figure 4.24	Seismic refraction tomography at Bukit Chondong, Beseri.	84
Figure 4.25	Inversion model resistivity of (a) Pole – dipole array and (b) Wenner – Schlumberger array at Bukit Chondong, Beseri.	85
Figure 4.26	Rock sample of (a) sandstone and (b) mudstone at Bukit Chondong.	86
Figure 4.27	Thin section photomicrographs of (a) sandstone and (b) mudstone.	86
Figure 4.28	Seismic velocity of various mudrocks.	88
Figure 4.29	Seismic velocity of various sandstone.	89
Figure 4.30	Resistivity values of various mudrocks.	90
Figure 4.31	Resistivity value of sandstone.	90

LIST OF SYMBOLS

A	Area
b	Klinkenberg slip factor (Pa)
c	constant
cm/s	Unit centimeter per second
d	Darcy
D	Flow rate diameter
H	Length read on flow meter
I	Current
k	Geometric factor
k_g	permeability to gas
k_l	permeability to liquid
K	Bulk modulus
km	Kilometer
km/s	Unit kilometer per second
L	Length of specimen
ℓ	Length
l	mean free path of the gas molecules (m)
m	Meter
m/s	Unit meter per second
p	pore pressure (Pa)
P_1	Absolute pressure bars
P_2	Pressure at which the flow rate
r	pore radius
R	Resistance
T	temperature (K)
t	time
V	Voltage
V_p	Velocity of P-wave
V1	Velocity of first layer
V2	Velocity of second layer
W_2	Weight in air

W_3	Weight in water
W_4	Weight of specimen after dried
z	Thickness
ρ_a	Apparent resistivity
κ	Boltzmann's constant (JK^{-1})
θ_{ic}	Critical angle of incidence
ρ_d	Density
ρ	Electrical resistivity
θ_i	Incidence angle
<	Less than
μd	microdarcy
>	More than
Ωm	Ohm-meter
%	Percent
μ	Shear modulus

LIST OF ABBREVIATIONS

BH	Borehole
C	Current electrode
CM	Chepor Member
CPT	Cone Penetration Test
DCPT	Dynamic Cone Penetration Test
EHR	Enhancing Horizontal Resolution
EM	Electromagnetic
ERT	Electrical Resistivity Tomography
ES	Electrode Selector
GPR	Ground Penetrating Radar
GRM	Generalized Reciprocal Method
HCS	Hummocky cross stratification
IP	Induced Polarization
KPF	Kubang Pasu Formation
NNW	North-northwest
P	Potential electrode
P-waves	Primary waves
RMS	Root Mean Square
RQD	Rock Quality Designation
SAS	Signal Averaging System
SF	Semanggol Formation
SP	Self Potential
SPT	Standard Penetration Test
SRT	Seismic Refraction Tomography
SSE	South-southeast
VES	Vertical Electrical Sounding
1-D	One Dimension
2-D	Two Dimension

PARAMETER GEOFIZIK BAGI BATUAN SEDIMEN DI BARAT LAUT SEMENANJUNG MALAYSIA

ABSTRAK

Kaedah geofizik kerap kali digunakan bagi mentafsir sifat bahan subpermukaan bumi. Julat besar bagi nilai halaju seismik dan keberintangan batuan menyebabkan kesukaran pengamal kejuruteraan bagi tujuan ini. Di Barat Laut Semenanjung Malaysia, lima kawasan dipilih bagi mengkaji seismik pembiasan tomografi dan keberintangan elektrik tomografi yang akan disepadukan bersama keporosan dan kebolehterlapan batu. Sampel batuan diambil di kawasan kajian bagi tujuan ujian makmal untuk mendapatkan nilai keporosan dan kebolehterlapan bahan batuan ini. Di Kedah, Formasi Semanggol di Bukit Kukus, Kuala Ketil meliputi fasies usia Perm; rijang dan batu lempung. Halaju seismik bagi fasies rijang adalah >1500 m/s dan nilai keberintangan 1400 – 45000 Ωm , manakala bagi batu lempung, 600 – 1200 m/s dan 400 – 1000 Ωm . Keporosan dan kebolehterlapan bagi rijang ialah 3% dan $2.05 \times 10^{-4} \mu\text{d}$ manakala batu lempung, kedua-dua sifat batu adalah tinggi disebabkan sifatnya yang rapuh. Fasies usia Trias bagi Formasi Semanggol terletak di kawasan Kulim – Baling dimana halaju seismik fasies rijang nipis >1400 m/s dan nilai keberintangan 5000 – 60000 Ωm . Di Perlis, anggota Chepor untuk Formasi Kubang Pasu terletak di Bumita Kuari, Utan Aji dan Bukit B, Guar Jentik. Ia meliputi batu lumpur merah, batu lumpur kelabu dan batu pasir. Halaju seismik bagi kedua-dua batu lumpur hampir sama berlainan dengan nilai keberintangan dimana batu lumpur merah memberi nilai rendah (10 – 150 Ωm) dan batu lumpur kelabu nilai yang lebih tinggi (120 – 500 Ωm). Nilai keporosan batu lumpur merah adalah 0.95% dan 1.9% untuk batu lumpur kelabu. Nilai kebolehterlapan bagi kedua-

dua batu lumpur memberikan nilai yang hampir sama. Formasi Kubang Pasu teratas di Bukit Chondong, Beseri terdiri daripada fasies berulang iaitu batu pasir dan batu lumpur. Halaju seismik bagi batu lumpur adalah 500 – 2500 m/s dengan nilai keberintangan 20 – 130 Ω m manakala bagi batu pasir adalah 4500 – 7000 m/s dengan nilai keberintangan 100 – 400 Ω m. Keporosan bagi batu lumpur dan batu pasir adalah 1.6% dan 0.9%, manakala kebolehterlapan kedua-dua batu adalah rendah dengan sedikit perbezaan, iaitu $8.82 \times 10^{-5} \mu$ d bagi batu lumpur dan $5.37 \times 10^{-4} \mu$ d untuk batu pasir. Maka, nilai geofizikal telah diwujudkan dan disepadukan bersama nilai keporosan dan kebolehterlapan batu. Hubungkait halaju seismik dan keberintangan daripada hasil kajian dengan nilai teori telah dicadangkan. Hasil kajian mendapati, jenis batuan endapan boleh dibezakan melalui kaedah geofizik khususnya keberintangan elektrik tomografi.

GEOPHYSICAL PARAMETERS FOR SEDIMENTARY ROCK IN NORTHWESTERN PENINSULA MALAYSIA

ABSTRACT

Geophysical methods have been utilized in studying the subsurface geology of the earth. Broad range of seismic velocity and resistivity values of rocks makes it difficult to interpret the type of subsurface material. In northwestern Peninsula Malaysia, five localities have been selected to conduct seismic refraction tomography and electrical resistivity tomography to be integrated with the porosity and permeability of rocks. The rock samples from the site were tested in laboratory to obtain its porosity and permeability. In Kedah, the Semanggol Formation at Bukit Kukus, Kuala Ketil consist of Permian facies; chert and claystone. The chert facies give seismic velocity of >1500 m/s and resistivity of 1400 – 45000 Ωm while claystone gives 600 – 1200 m/s and 400 – 1000 Ωm respectively. The porosity and permeability of chert is 3% and 2.05×10^{-4} μd while for claystone, both properties are high due to its friable characteristics. The Triassic facies of Semanggol Formation located in Kulim – Baling area where thinly chert facies characterized by seismic velocity of >1400 m/s and resistivity 5000 – 60000 Ωm . In Perlis, the Chepor Member of Kubang Pasu Formation is located at Bumita Quarry, Utan Aji and Hill B, Guar Jentik. It consists of red mudstone, grey mudstone and sandstone. The red mudstone and grey mudstone gives nearly the same seismic velocity. Unlike resistivity value, where red mudstone with low resistivity value (10 – 150 Ωm) and grey mudstone gives higher resistivity (120 – 500 Ωm). The porosity value for red mudstone is 0.95% and 1.9% for grey mudstone. The permeability value of both mudstones shows nearly the same value. The uppermost Kubang Pasu Formation at

Bukit Chondong, Beseri consists of repetitive facies of sandstone and mudstone. The mudstone exhibit velocity of 500 – 2500 m/s and resistivity of 20 – 130 Ω m, whereas sandstone velocity is 4500 – 7000 m/s and resistivity from 100 – 400 Ω m. The porosity value of mudstone and sandstone is 1.6% and 0.9% respectively. While permeability for both facies is low with a slight difference in value, mudstone with 8.82×10^{-5} μ d whereas sandstone with 5.37×10^{-4} μ d. Hence, the geophysical values were established and integrated with the values of porosity and permeability of rocks. Comparison of seismic velocity and resistivity values in these findings with theoretical values were suggested. This study suggested, the type of sedimentary rocks can be differentiated with the geophysical methods especially using electrical resistivity tomography.

CHAPTER 1

INTRODUCTION

1.0 Background

The complexity of the earth due to inhomogeneity obstructs the ability to explore its resources maximally. Hence, it is important to understand the physical and chemical properties of the earth in great extents for the comprehensive study of the subsurface and its constituents. Exploring the Earth's interior using geophysical methods involves taking measurement at or near the surface of the earth. The results from geophysical analysis can give both vertical and lateral variations of the physical properties of the Earth's subsurface. One of the physical properties that can be measured are the porosity and permeability of rocks. These properties are very important in earth exploration especially in the oil and gas sector.

There are many reasons for studying sedimentary rocks, not least because of the wealth of economic minerals and materials contained within them. Sedimentological and petrological techniques are increasingly used in searching for natural resources. Sedimentary rocks supply much of the world's iron, potash, salt, building materials and many other raw materials (Tucker, 1981).

1.1 Sedimentary rock

Some of the earth's surface is sedimentary in origin and these include the common sandstones, limestones and shales and the less common ironstones, coal and

chert. Sedimentary rocks are formed through several processes; physical, chemical and biological processes. There are two categories of sedimentary rocks based on its origin which relates to this research shown in Table 1.1. Terrigenous sediments are those consist of fragments from pre-existing rocks that have been transported and deposited by physical processes. Sediments primarily of biogenic or biochemical are cherts and limestones (Tucker, 1981).

Table 1.1: Groups of sedimentary rock (Tucker, 1981).

Terrigenous sediments	Biogenic sediments
Sandstones, mudrocks, conglomerate and breccias.	Cherts, limestones, coal and oil shale.

1.2 Problem statement

Northwestern of Peninsula Malaysia has one of the interesting geological features and age that consists of various earth formations resulting from geological events which has occurred million years ago. Researchers especially geologist interpret the geological structure and geomorphology based from the analysis of exposed bedrock or outcrop exist at the earth surface (Lisle, 2004). The characterization of actual rock type that exist at the subsurface only by observation is difficult and not precise. Therefore, to obtain a more accurate result, geologist applied logging tools which provide useful information to study the subsurface lithology (Keys, 1997). Logging tool is an expensive tool and difficult to conduct in remote areas. Moreover, logging only provide information of the lithology at a single point.

In suburban area, the community usually built houses on their own land without knowing the type of rock foundation and properties lies beneath their house.

If a house is wrongly build on an unsuitable rock foundation, the house might collapse or cracks developed. Imaging the subsurface is important to determine the type of rock present at the area before building any structure.

The seismic velocity and resistivity range established by various geophysicists gives a wide range of values subject to the type of rocks. A type of rock having different type of facies will have its own specific range of values. Having a smaller range of values would help researchers to interpret the type of rock in a specific way thus accurately.

1.3 Research objectives

The objectives of this study are as follows.

1. To characterize the geological outcrop in northwestern Peninsula Malaysia using geophysical methods; seismic refraction tomography and electrical resistivity tomography.
2. To compare geophysical results; seismic velocity and resistivity values with the rock properties (porosity and permeability) of northwestern Peninsula Malaysia.
3. To determine the seismic velocity and resistivity values of geological formation in northwestern Peninsula Malaysia.

1.4 Scope of the study

This research is conducted in northwestern Peninsula Malaysia, specifically in Kedah and Perlis during hot and dry season. The study area consists of interesting

and complex geological structure to conduct seismic refraction tomography (SRT) and electrical resistivity tomography (ERT). There are many geological formations which exist in Kedah and Perlis, three types of formation are included in this study; Semanggol Formation, Chepor Member and uppermost Kubang Pasu Formation. The geophysical survey is carried out on top of the geological outcrops as a guide to correlate with the geophysical results. The application of geophysical methods allows the seismic velocity and resistivity distribution of the subsurface to be extracted for research use. For further research, rock samples from the site are taken for specimen observation and laboratory test. The parameter selected for laboratory test are porosity and permeability. Later, the porosity and permeability of rocks are integrated with the seismic velocity and resistivity values. Some of the rock samples were sent to the Department of Mineralogy and Geosciences, Ipoh for petrographical analysis.

1.5 Novelty of the study

The first novelty of this research is the correlation of seismic refraction tomography and electrical resistivity tomography in studying the outcrop. There are some cases on which one of the geophysical tools is unsuitable to apply depends on the geological condition. Therefore, this research reveals which of the geophysical tools can map better the outcrop.

The second novelty arise from the range values of seismic velocity and resistivity specifically for geological formation in northwestern Peninsula Malaysia. It has been known that the table of seismic velocity and resistivity of rocks developed by previous geophysicists give a broad range of values with respect to the

type of rock. At the end of this study, the different type of sedimentary facies will exhibit its specific range of seismic velocity and resistivity values.

1.6 Thesis layout

This section describes the arrangement of the thesis as follows.

Chapter 2 mainly discussed about the theory of seismic refraction tomography (SRT) and electrical resistivity tomography (ERT) in details. The types of seismic waves and how it propagates with included figures and equations are stated for better understanding in seismic refraction. Explanation for electrical resistivity on how the current travels through the subsurface thus creating potential is stated. There are eight common arrays in ERT but only two are used in this study. Details regarding porosity and permeability are stated and continue to the previous studies related to this research.

Chapter 3 discussed the methodology of this research. Flow chart of the whole research is visualized. The geology of northwestern Peninsula Malaysia is discussed with the geological formations related in this study. The study area for five survey localities are stated accordingly. Next, the geometry of data acquisition for both SRT and ERT is explained. Continue to data processing of SRT and ERT raw data using respective software. The methodology to conduct porosity and permeability test are explained with the illustrations of equipment. The equations to get the result of porosity and permeability of rock are stated.

In Chapter 4, the tomogram result of SRT and ERT with the outcrop are showed. The arrangement of the results at each site survey are according to the

geological formations. The results of porosity and permeability are tabulated with the geophysical results. Explanations and interpretations with thin section photomicrographs are included. At the end, the results of both seismic velocity and resistivity values in these findings are compared with the theoretical values and is graphically presented.

Chapter 5 states the conclusion of this research. Recommendations and improvements for future studies are also suggested.

CHAPTER 2

LITERATURE REVIEW

2.0 Introduction

Outcrop can be defined as a visible exposure of bedrock on the earth surface. In northwestern Peninsula Malaysia, most of the outcrop are covered by vegetation but some are visible due to the activity of mining. The presence of outcrops allows observation and sampling of the bedrock for petrophysical analysis. Petrophysical analysis in this research comprises of porosity and permeability of rock. The petrophysical result is then integrated with the geophysical parameter. In this study, seismic refraction tomography (SRT) and electrical resistivity tomography (ERT) methods are applied on top of the outcrop at two locations in Kedah and three locations in Perlis. SRT is based on stress and strain concept. Stress is applied to an elastic medium, the energy transmitted to the Earth will be in the form of elastic waves and travels through or at the surface of the Earth as seismic waves (Kearey et al., 2002). ERT uses resistivity properties of materials as its parameter. In determining the subsurface resistivity distribution, current is injected through the ground from two current electrodes and measuring the resulting voltage difference at two potential electrodes (Loke, 1999).

2.1 Seismic refraction tomography theory

Seismic refraction tomography (SRT) uses propagation of waves through the earth. The propagation of waves depends on the elastic properties of the rocks.

(Telford et al., 1990). The basic principle of seismic exploration consists of generating seismic waves and measuring the time required for the waves to travel from the sources to a series of geophones, usually along a straight line directed toward the source (Figure 2.1).

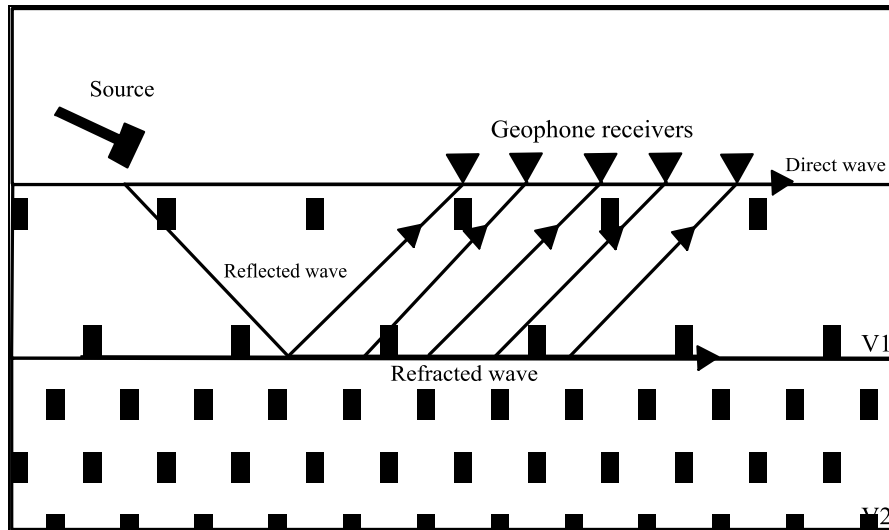


Figure 2.1: Ray paths for seismic waves.

In the history of seismic imaging, most survey has used only compressional waves due to it simplifies the survey technique in two approaches (Kearey et al., 2002). Firstly, the detectors of seismic survey only record the vertical ground motion and less concern to the horizontal motion of S-waves. Secondly, it is easy to recognize since the higher velocity of P-waves always reach the detectors before any related S-waves. It utilizes the principal of elastic waves travelling with different velocities at different formation of the Earth. The velocity of the seismic waves is determined by Elastic Moduli and the densities of materials through which they travel. For seismic refraction to work, the sound velocity in deeper layer must be greater than the layer above it. As this condition is encountered, the refracted waves arrive at the Earth's surface where it can be noticed by a geophone which generates an electrical signal and sends the signal to a seismograph (Haeni, 1986).

P-waves or compressional waves refer to the particle movements back and forth along the direction and parallel to wave's propagation. The particle motions that transmit longitudinal waves consist of a series of dilations and compressions that envisioned as the centers of rock particles being moved closer than normal and then moved farther apart than normal (Figure 2.2). P-waves are also referred to as compressional waves due to the particle compressions during their transport.

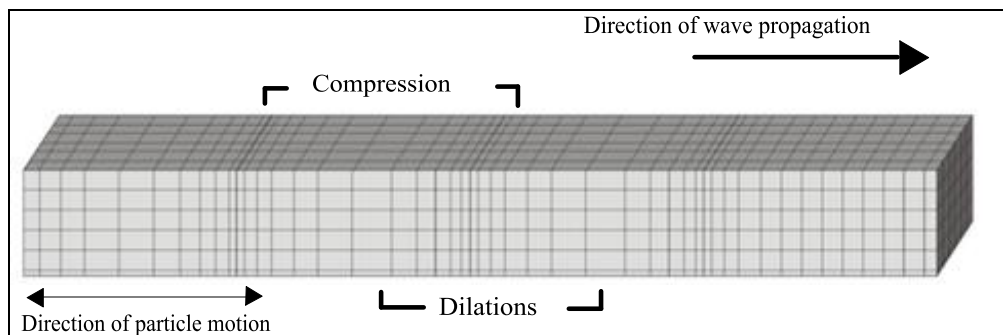


Figure 2.2: Compressional and dilation due to ground particle motions.

P-waves have the greatest speed and therefore appear first on traces at the seismograph. Velocity of P-waves (V_p) is given by Equation 2.1.

$$V_p = \left[\frac{K + \frac{4}{3}\mu}{\rho_d} \right]^{1/2} \quad (2.1)$$

Where;

K: Bulk modulus

μ : Shear modulus

ρ_d : Density

Acoustic energy is generated to the ground surface by an energy source as a sledgehammer impacting to a metallic plate during seismic refraction survey. The acoustic waves propagate through the subsurface of the ground at varies velocities

influenced by the elastic properties of the material through which they travel. When the waves reach at the interface where the velocity is change significantly, some of the waves is reflected to the surface and some is travelled into the lower layer where the velocity at the lower layer is higher than the upper layer. Some of the energy also critically refracted along the boundary line between two layers of rock. Critically, refracted wave propagates along the boundary line at the velocity of the lower layer and continually refract energy back to the surface. The receiver then records the incoming refracted and reflected waves (Redpath, 1973). The time-distance plots of this first arrival are interpreted to derive information on the depth to refraction interfaces. Figure 2.3 shows the mechanism of seismic refraction.

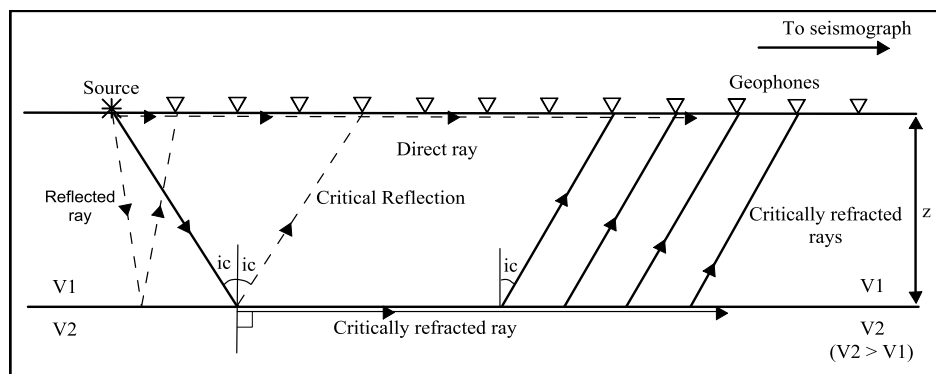


Figure 2.3: Diagrammatic of SRT (Modified from Redpath, 1973).

The seismic velocities in rock materials depend on several factors particularly rock type, density, grain size and shape, porosity, anisotropy, pore of water, clay content, confining pressure and temperature. Furthermore, weathering, bedding planes and properties of joint (filling material, dip and strike) have significance influence on the seismic velocity (Kahraman, 2001). Post formational processes such as structural deformation, fracturing and weathering decrease velocity although thermal re-crystallization will increase rock strength and velocity. Due to these

factors, seismic velocities in shallow earth materials are highly variable. Table 2.1 shows the seismic velocity of sedimentary rock.

Table 2.1: Seismic velocity table of sedimentary rock (Reynolds, 1997).

Sedimentary Rocks	Seismic velocity (m/s)
Sandstone	1400 – 4500
Clay	1000 – 2500
Shales	2000 – 4100

2.2 Electrical resistivity tomography theory

The aim of ERT is to determine the subsurface resistivity dispersal by making measurements on the ground surface. Based on the measurements, the true resistivity of the subsurface can be roughly calculated. The resistivity value depends on the geological parameter such as degree of water saturation, degree of fracturing, concentration of dissolved salts, porosity and physical composition (Pokar, 1998). It is a non-destructive method which allows the imaging of outcrops distinguishable vertically and horizontally.

The ERT works through the measurement of potential difference at points in the earth that is produced by injecting current through the ground. Ohm's law (Equation 2.2) state that current is directly proportional to voltage and inversely proportional to resistance (Burger, 1992).

$$I = \frac{V}{R} \quad (2.2)$$

Where;

I: Current; V: Voltage; R: Resistance

Various geologic materials should have different resistance to current flow, from the value of current and voltage, resistance is measured thus subsurface medium can be determine. Resistivity of a material is defined as the resistance between two opposite faces of a unit cube of a material. Figure 2.4 shows a cylinder with resistance, R while resistivity depends on the length and cross-sectional area, given Equation 2.3 and 2.4 (Kearey and Brooks, 1991).

$$R = \rho \frac{\lambda}{A} \quad (2.3)$$

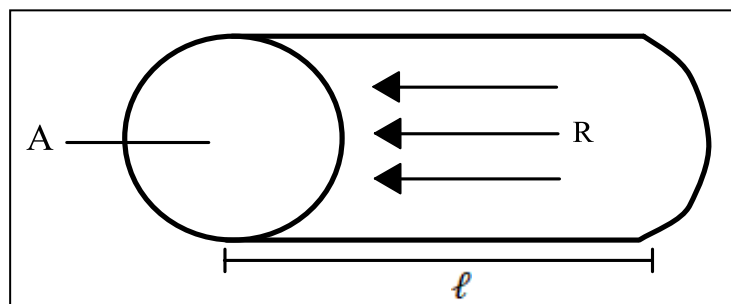


Figure 2.4: Electrical resistivity with relation of resistance (R), area (A) and length (l).

Rearranging the formula, resistivity can be written as

$$\rho = \frac{RA}{\lambda} \quad (2.4)$$

Where ρ is electrical resistivity (Ωm)

The resistivity measurements are basically made by injecting current into the ground through two current electrodes, C1 and C2 thus resulting potential difference will be picked by two potential electrodes, P1 and P2 as shown in Figure 2.5.

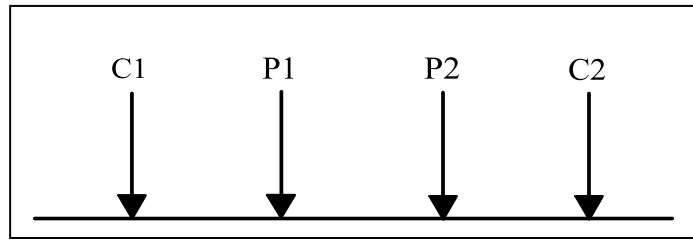


Figure 2.5: Four electrode array to measure the subsurface resistivity (Loke, 1999).

The apparent resistivity, ρ_a is calculated from the value of current, I and voltage, V using Equation 2.5.

$$\rho_a = k \frac{V}{I} \quad (2.5)$$

Where;

k : geometric factor

ρ_a : apparent resistivity

Resistivity meter usually give the resistance, $R = V / I$; therefore, substituting into Equation 2.5, it will become

$$\rho_a = kR \quad (2.6)$$

The apparent resistivity is calculated from Equation 2.6. It measures the resistivity of a homogenous ground which will give the same resistance value for the same electrode arrangement. The relationship between apparent resistivity and the true resistivity is quite complex, therefore an inversion of the measured apparent resistivity is made to determine the true subsurface resistivity using a computer software.

Figure 2.6 shows the illustration of current flow in homogeneous subsurface. When current is injected into the ground by two current electrodes, the current flows radially away from the electrodes and between the electrodes. Potential differences

between two potential electrodes are measured by voltmeter. The bigger the electrode spacing, the deeper the current will flow.

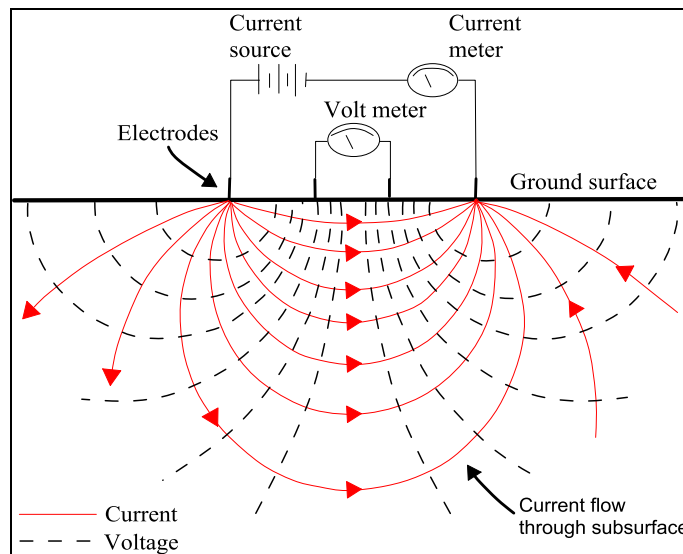


Figure 2.6: Current is induced between paired electrodes (red lines). Potential difference between paired voltmeter electrodes is measured (after Anderson and Croxton, 2008).

Electrical resistivity value of Earth's matter shows a greatest variation for all rocks and minerals. It has a much larger range compared to other physical quantity produced by other geophysical methods. Table 2.2 shows the resistivity of common sedimentary rock.

Table 2.2: Resistivity table of sedimentary rock (Loke, 1999).

Sedimentary Rocks	Resistivity (Ωm)
Sandstone	$8 - 4 \times 10^3$
Shale	$20 - 2 \times 10^3$
Limestone	$50 - 4 \times 10^2$

2.3 Porosity and permeability

Quantification of void space is called as the porosity of rock whereas the measure of the ability of rock to channel fluids is called the permeability. Studying these two types of rock properties is essential before dealing with the types of fluids, amount of fluids, rates of fluid flow and fluid recovery estimates can be predicted. The texture of sedimentary rock is determined chiefly by grain shape and roundness, grain size and sorting, grain orientation and packing and chemical composition (Tiab and Donaldson, 2015).

2.3.1 Porosity

Porosity can be clarified as the void fraction of rock also known as pore spaces. To calculate the numerical value of porosity for a rock, its pore space volume should be divided to its bulk volume. The most accepted method to measure the porosity of rock is by laboratory test using mercury injection technique, but this technique is time consuming, expensive and tedious to use (Ghiasi-Freez et. al., 2014). The factors relating to the magnitude of porosity in clastic sediments are as follows:

1. Constancy of grain size: Uniformity or sorting is the gradation of grains. If small particles of silt or clay are mixed with larger sand grains, the effective (interconnecting) porosity will be considerably reduced. There are four major factors which affect the sorting; the size range of material, depositional setting, current characteristics and the period of the sedimentary process.

2. Degree of cementation or consolidation: The highly cemented sandstones have low porosities, opposite to unconsolidated rocks which is soft, have high porosities. Cementation takes place during lithification and rock alteration by circulating groundwater. The process is essentially filling void spaces with mineral material, which reduce porosity. The cementing substance include calcium carbonate, iron sulfides, limonite, hematite, dolomite, calcium sulfate, clays and many other materials including any combination of these materials.
3. Amount of compaction during and after deposition: Compaction tend to lose voids and squeeze fluid out to move the mineral particles close together, particularly the fine-grained sedimentary rocks. Whereas compaction is an important lithifying process in claystones, shales and fine-grained carbonate rocks. It is minimal in closely packed sandstones or conglomerates. Generally, porosity is lower in deeper and older rocks, but exceptions to this basic trend are common. Mostly carbonate rocks show little evidence of physical compaction.
4. Forms of packing: The increase overburden pressure, poorly sorted angular sand grains show a continuous change from random packing to a closer packing (Tiab and Donaldson, 2015).

2.3.2 Intrinsic permeability

Permeability or intrinsic permeability portray a mobility of fluid within porous rock materials involving pore geometry of rocks itself (porosity, pore shape and pore size distribution). Sedimentary units which consist of major clay are

commonly barely permeable parts of groundwater flow system. Permeability is an important parameter to control the fluid flow systems at depth, it is wide in ranges from 10^{-12} to less than 10^{-23} m² for diverse rock type and depth condition (Neuzil, 1994). Many sedimentary rocks show great anisotropy in permeability and sensitive to cracks and fractures. Predicting permeability from other physical properties such as porosity and grain size is arduous because of the complexity of the relationship.

Permeability measurements under high confining pressure can be done in a laboratory to predict the permeability structure at depths. One of the simple methods for measuring permeability is by steady state method utilizing gas as a pore fluid which gives the following advantages: (1) Commercial gas flow-meters that cover wide range of flow rate for any kind of gas to measure wide range of permeability quickly and accurately. (2) Nitrogen is chemically inert and it is only necessary to consider the mechanical effects for the permeability changes with an increase of confining pressure. (3) Gas is least sensitive to temperature change which may reduce or lessen the error for permeability measurement compared to water (Tanikawa and Shimamoto, 2006). Throughout this research, the permeability values are presented in microdarcies. The SI unit for permeability is square meter and 1 darcy = 0.9869×10^{-12} m². It can be assumed that permeability was measured with an air permeameter at low confining pressures, without Klinkenberg correction (Nelson, 1994).

2.3.3 Klinkenberg effect

Klinkenberg (1941) findings was the permeability to gas is relatively higher than water. This occurrence is called the “slip flow” between solid walls and gas

molecules. Gas molecules strike one another and to pore-walls during in motion through the pore medium. When the pore radius reaches to the mean free path of gas molecules, the frequency of collision between gas molecules and solid walls increases. Therefore, this additional flux due to the gas flow at the wall surface becomes effective to enhance the flow rate. This phenomenon is called Klinkenberg effect and its effect is expressed as Equation 2.7 (Tanikawa and Shimamoto, 2006).

$$k_g = k_l \left(1 + \frac{4cl}{r} \right) = k_l \left(1 + \frac{c\kappa}{\pi\sqrt{2}r^3} \frac{T}{p} \right) = k_l \left(1 + \frac{b}{p} \right) \quad (2.7)$$

Where;

k_g : permeability to gas

k_l : permeability to liquid

l : mean free path of the gas molecules (m)

r : pore radius

κ : Boltzmann's constant (JK^{-1})

T : temperature (K)

c : constant

p : pore pressure (Pa)

b : Klinkenberg slip factor (Pa)

2.4 Previous study

Research done previously which related to this study were discussed according to the divided sections.

2.4.1 Integration of geophysical and geotechnical survey

Edy et al. (2015) investigated the relationship between seismic refraction tomography (SRT) and borehole logging in a granitic area at Ulu Tiram, Johor. Three lines of seismic survey were conducted to analyze the subsurface for quarry

development. Along the seismic line, two boreholes were drilled to obtain the relationship between both methods. There are 3 distinct velocity layers can be found on both borehole (BH) records as shown in Figure 2.7. The seismic survey results were assessed along with standard penetration test (SPT) and rock quality design (RQD) information. The correlation of SRT and BH data can be used for better subsurface characteristics exploration thus providing data rapidly at a relatively low cost and give benefits in terms of work time.

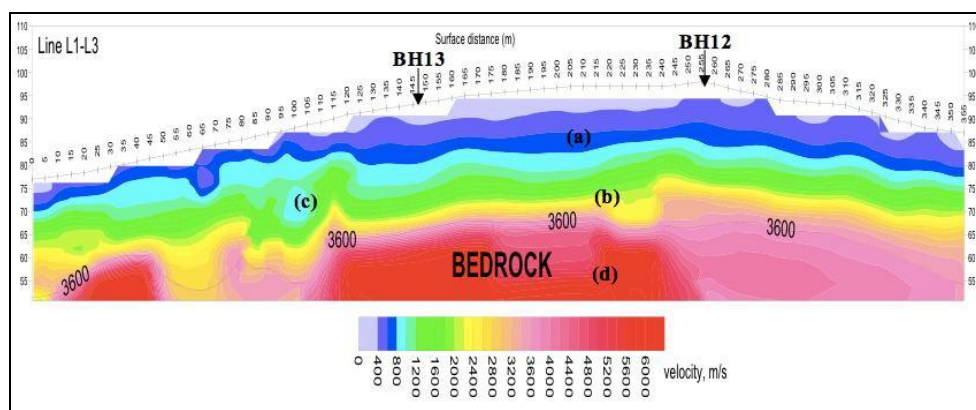


Figure 2.7: Seismic section at Ulu Tiram, Johor (Edy et al., 2015).

Ozcep et al. (2009) used artificial intelligent approaches to get better results from conventional technique system to compare water content of soils obtained from electrical resistivity tomography (ERT). The variables for this system are the water content laboratory measurements and the ERT reading. The output variable is water content of soils. The research clustered 148 data sets into 120 training sets and 28 testing sets for developing the fuzzy system and verifying the ability of the system prediction respectively. Soil is a heterogeneous medium consisting of liquid, solid and gaseous phase. In soil, spontaneous electrical phenomena and in behavior of electrical fields which artificially created in soil, the solid and liquid phase plays an essential role. The study area is in Istanbul (Yesilkoy, Florya and Basinkoy) and Golcuk. The electrical resistivity is measure by vertical electrical sounding (VES) in

many points of these locations by field resistivity equipment. In geotechnical prospects, the soil samples from borings, soil mechanics laboratory were applied to determine the soil water contents from these samples. The relationships between soil water content and electrical parameters were obtained by curvilinear models (Figure 2.8). The artificial intelligent system such as artificial neural networks, Fuzzy logic applications, Mamdani and Sugeno approaches based on some comparisons about interconnection between electrical resistivity and soil water content for Istanbul and Golcuk soils in Turkey was constructed for identifying water content with electrical resistivity of soils.

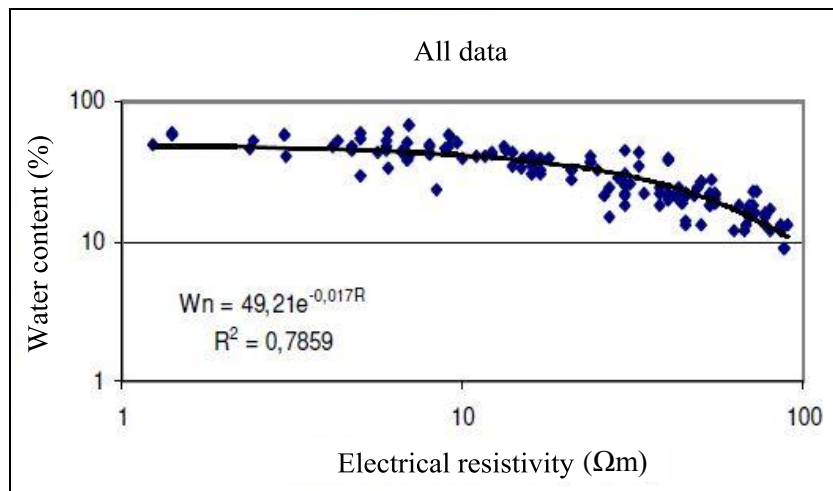


Figure 2.8: Relationship between soil electrical resistivity with water content for all data (Ozcep et al., 2009).

Cosenza et al. (2006) applied geophysical and geotechnical survey at Garchy (Nievre, France) to construct qualitative and quantitative correlations between ERT and geotechnical data in a simple geological context. Geotechnical tests and ERT sections with reference to qualitative correlations were consistent with a three-layer model; a fine soil with a significant clay fraction sandwiched between oolitic limestones and a low moisture sandy soil. This research certifies the correlations between ground penetrating radar (GPR) profiles reflectors with the variations of

vertical geotechnical property mainly due to vertical water content changes. On the other hand, there were no clear observed relationship between cone resistance and inverted resistivity extracted from ERT sections. The inverted resistivity values obtained from 1-D sounding were considered thus enhanced the lithological discrimination. Moreover, a satisfactory quantitative correlation between measured water content and inverted resistivity values has been obtained (Figure 2.9). This correlation demonstrates once more that resistivity is a good indirect predictor of water content.

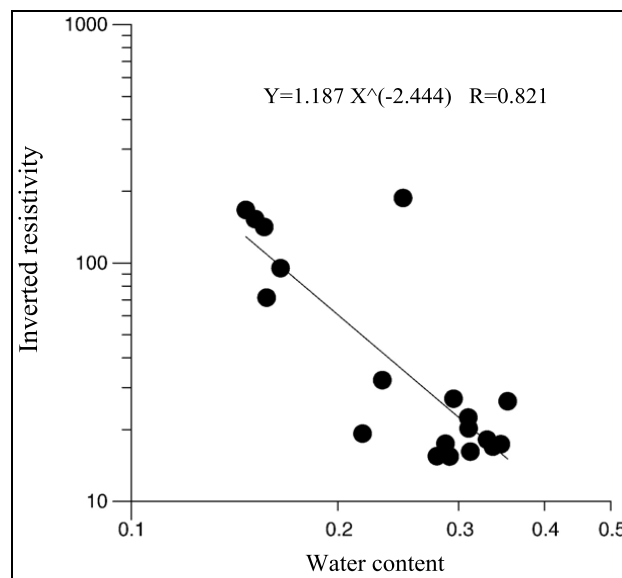


Figure 2.9: Correlation between measured water content and inverted resistivity (Cosenza et al., 2006).

It is difficult to estimate the in-situ porosity and water saturation for shallow subsoil. Ghose and Slob (2006) relate SRT and GPR reflection coefficients to porosity and water saturation using a shared earth model to integrate quantitatively SRT and GPR angle dependent reflection coefficients. This new approach has been tested through numerical simulations which clearly showed from either SRT or GPR data, it is impossible to obtain unique estimates for porosity and water saturations,

however a correct integration of those two data types leads to unique and stable estimates at a subsoil layer boundary.

Rahmouni et al. (2013) used P-wave velocity (V_p) to determine the geotechnical properties of rock materials. The P-wave velocity of a rock is closely related to the intact rock properties. To predict the porosity and density of calcarenite rocks that were characterized as historical monument, the use of a simple ultrasonic velocity was applied. The ultrasonic test is based on measuring the propagation time of a P-wave in the longitudinal direction. The results show good correlations between V_p , porosity and density indicating P-wave is an appropriate technique to estimate the porosity and density (Table 2.3).

Table 2.3: Physical properties of calcarenite rocks.

Sample	V_p (km/s)		Density (g/cm^3)		Porosity (%)
	Dry	Saturated	Dry	Saturated	
1	3.8	3.84	1.75	2	25.69
2	3.7	3.74	1.68	1.97	29.82
3	3.62	3.69	1.64	1.95	31.07
4	3.64	3.62	1.59	1.92	33.50
5	3.61	3.65	1.6	1.95	35.07
6	3.56	3.59	1.6	1.94	35.83

Sudha et al. (2008) associates ERT with Standard Penetration Test (SPT) and Dynamic Cone Penetration Test (DCPT) for geotechnical investigations at two sites. The site was at thermal power plants in Uttar Pradesh, India. Both SPT and DCPT tests were conducted at 28 points and two ERT profiles each measuring 355 m long using 72 electrodes at 5 m spacing. Using borehole data and grain size analysis of soil samples collected from boreholes, the electrical characterization of subsurface soil was achieved. To correlate the transverse resistance of soil with the number of

blow counts (N-values) acquired from SPT and DCPT data, the concept of electrical resistivity variation with soil strength related to the grain size distribution, cementation, porosity and saturation has been used. Based from observation, the transverse resistance of soil column is linearly related with the number of blow counts (N-values) at these sites. The linear relationships are site-specific and the coefficients of linear relation are sensitive to the lithology of subsurface formation, which was verified by borehole data. The study signifies the usefulness of the ERT method in geotechnical investigations which are economic, efficient with less time consuming compared to other geotechnical methods such as SPT and DCPT.

Oyedele et al. (2011) aimed to image shallow subsurface with a view to evaluate the stratigraphy and competency of the shallow formation as foundation materials at Ilkoyi, Lagos, Nigeria. Integrating geophysical survey (Vertical Electrical Sounding) and geotechnical survey (CPT and SPT), both survey showed good agreement. Four to five subsurface layers were delineated within the study area thus showing good correlation with the soil layers in bore logs. The existence of loose sand, peat and clay near the surface capable of degrading building structures. The subsurface layers up to 16 m depth are mechanically unstable with low penetration resistance value which may not serve as good foundation materials. Shallow foundation is unsuitable for building as structures to build in this area should be safely founded in competent and mechanically stable coarse sand through piling.

Muthukrishniah et al. (1995) objective is to develop the relationships between geophysical and geotechnical properties of marine sediments by experimental and theoretical methods from the east (Madras) and the west (Cochin) coasts of India. In the experiment, several types of geophysical properties of the sediment, acoustical and electrical properties were measured. The acoustical electrical and the

geotechnical properties was correlated by conducting experiments with the help of modified consolidometer. Biot-Stoll model was used to predict the permeability with the use of geophysical and geotechnical parameters. The permeability predicted from the model agrees quite well with the measured values for both clays tested. The Biot-Stoll model underestimates the coefficient of permeability by 40% at a porosity of 0.6659, this lessens to about 3% at a porosity of 0.5506 for Cochin clay. Considering that the permeability of clays varies in the order of 10^{-7} to 10^{-9} cm/s, even 40% variation will show relatively small for permeability. Moreover, the results show that correlations can be made between acoustical (compressional wave velocity), electrical (formation factor) and various geotechnical properties.

2.4.2 Geophysical survey

Griffiths and Barker (1992) applied ERT and modelling in complex geological area in Staffordshire, England. This study used Wenner array with up to 32 electrodes connected through a multicore cable to a computer controlled switching module and a resistivity meter. The capabilities and limitations of the technique was illustrated by a series of computed constant separation traverses for models of simple subsurface structures. In many conditions, the method provides an approximately true geoelectric cross-section of the subsurface beneath the profile. Additional information relating local lithology to the electrical imaging can be converted to geological section (Figure 2.10). It is concluded that with the equipment and software so far developed, good approximations to the true ERT sections can be acquired at depth between 100 and 200 m.

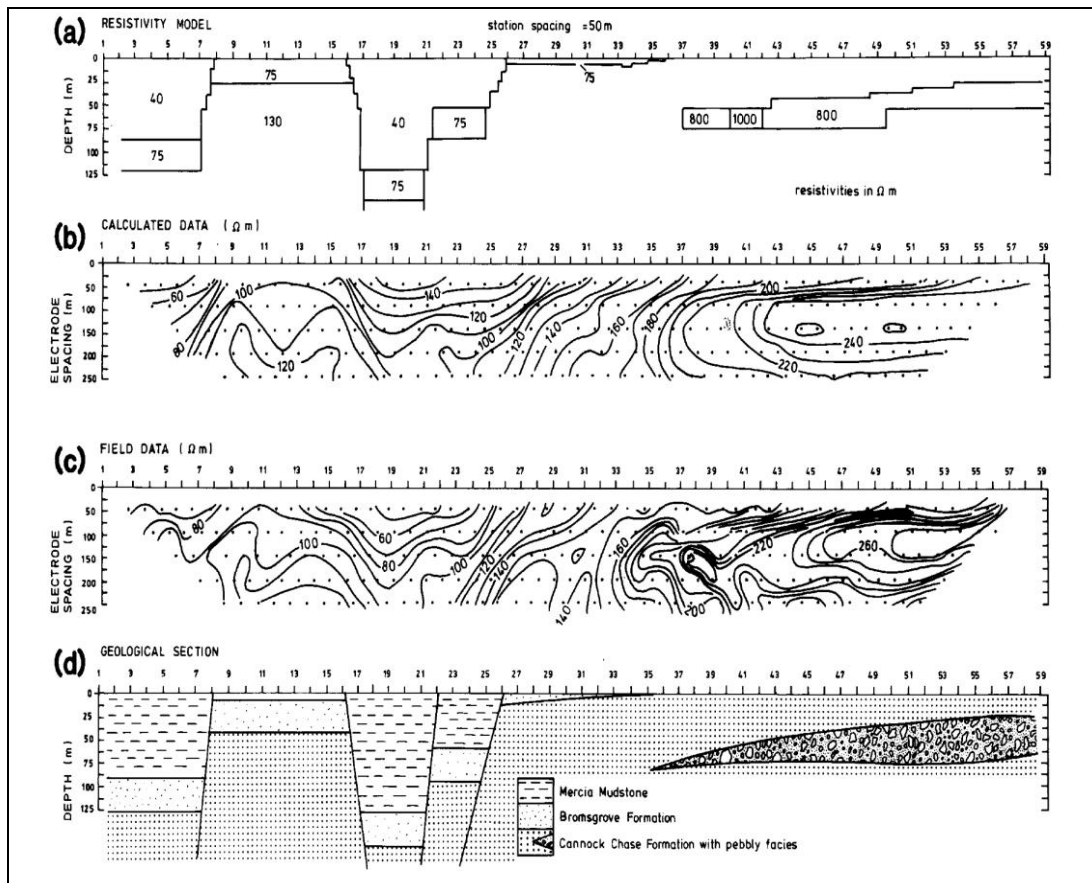


Figure 2.10: Interpretation of a faulted sequence in Staffordshire. (a) 2-D model. (b) Computed apparent resistivity pseudosection. (c) Field data. (d) Geological interpretation based on (a) and additional information (Griffiths and Barker, 1992).

Ismail et al. (2013) applied seismic refraction tomography for site characterization at Kaki Bukit, Perlis. The survey was done on top of the limestone outcrop. There are 3 parallel seismic lines conducted with 2 m geophone spacing. The results show that there are 4 main layers with velocity increases decently (Figure 2.11). The first layer is the top soil with velocity 300 – 500 m/s. The second layer is highly weathered limestone ranging from 500 – 800 m/s. The third layer shows highly fractured limestone giving seismic velocity from 800 – 1500 m/s. Lastly, the fourth layer is the bedrock limestone with >2000m/s seismic velocity. Thus, by conducting SRT, the bedrock formation, velocity distribution and depth underlying layers can be acquired in detailed.

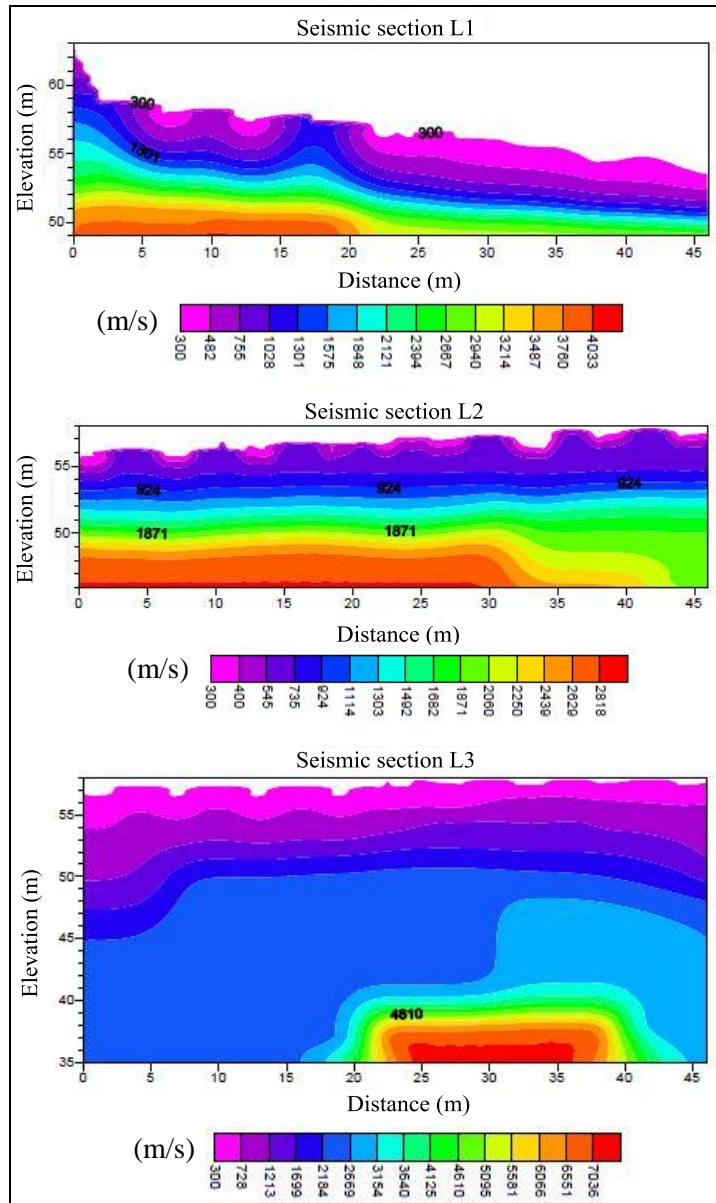


Figure 2.11: Seismic section of three lines at Kaki Bukit, Perlis (Ismail et al., 2013).

Muztaza et al. (2013) used electrical resistivity tomography with Enhancing Horizontal Resolution (EHR) technique to map shallow subsurface geology at Nusajaya, Kaki Bukit and Masai. The array applied was Pole – dipole with minimum 2 m electrode spacing. The inversion model at Nusajaya, Johor shows sandstone contain iron mineral (30 – 250 Ωm) and weathered sandstone (500 – 1000 Ωm). At Beseri, Perlis there are 3 different layers with resistivity values from 1 -50 Ωm denoted as clay, 125 – 500 Ωm indicating weathered limestone and 1200 – 3000 Ωm

is the limestone (Figure 2.12). The granitic area at Masai, Johor consist of two main zones. Resistivity value $<700 \Omega\text{m}$ is the granitic boulders and $>1000 \Omega\text{m}$ is the fractured granitic bedrock. The stratigraphy of the sedimentary, limestone and granite is successfully mapped using electrical resistivity tomography with EHR technique.

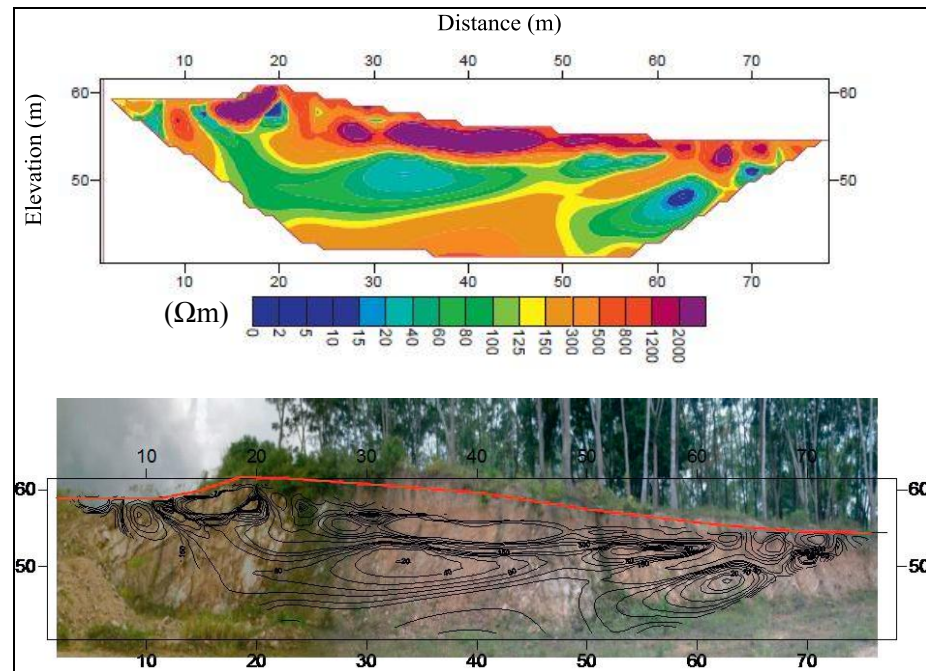


Figure 2.12: ERT at limestone area in Beseri, Perlis (Muztaza et al., 2013).

2.4.3 Geological study

Zaiton et al. (2009) carried out a geological research of a small hill at Bukit Kukus in the region of Kuala Ketil town which exposed the chert unit of the Semanggol Formation consisting black mudstone, tuffaceous sandstone, sandstone, tuff, paraconglomerate, siliceous shale and chert. At the same orientation fault plane, both thrust and normal faults lie. The dextral faults occupy the same alignment as the Bok Bak fault which is of sinistral. As the result of transpressional deformation northward thrusts occupy fault planes which were formally the normal faults. The

normal faults are the extensional faults occurring from the sinistral movement of the Bok Bak fault. The northward thrust is generated from the dextral movement along the northwest and west-northwestern faults, and is clarified to be the youngest fault movement onshore.

Basir and Zaiton (2007) studied the stratigraphy and sedimentology of the chert unit of Semanggol Formation by the distribution of rocks, their age and relationship among the units in the formation. There are five Permian and four Triassic radiolarian biozones recognized. The discovery of Permo-Triassic radiolarian faunas marks the chert unit is partly identical in age to the rhythmite and conglomerate units. Chert unit of Semanggol Formation is divided into eight sedimentary facies, which were deposited in an open-deep marine surrounding under the influence of different transport processes. Evidently there were widespread volcanogenic sediments proceeding to the deposition of the chert in the Semanggol Formation.

Detailed facies analysis of Semanggol Formation was done by Baioumy and Ulfa (2016) at Bukit Kukus and Baling areas, South Kedah. In this study, four facies from the Permian part were discovered at Bukit Kukus section including laminated black mudstone, interbedded mudstone and sandstone, volcanogenic sediments and bedded chert. The Triassic part of the formation is situated in Baling area. It is classified into three members. The lower member consists of claystone and bedded chert facies whereas the middle member encompassed sandstone and claystone interbeds (rhythmite). Next, the upper member is grouped into two main units; lower units and upper units. The lower unit is claystone and covers two facies, varve-like laminated silt and clay and massive black claystone. The upper unit is the various sandstone lithofacies stretching from hummocky cross stratified (HCS) sandstone to

thinly laminated sandstone to burrowed sandstone facies. Overall, the facies involved might represent the Permian-Triassic boundary section.

Meor and Lee (2004) studied the depositional environment of the Mid-Paleozoic red beds at Utan Aji, Perlis and its bearing on global eustatic sea level change. The Late Devonian to Early Carboniferous red colored mudstones and sandstones are widely distributed in northwest of Peninsula Malaysia. A complete and preserved sequence is exposed at Bumita Quarry, Utan Aji, Perlis and is described herein. The facies related are indicative of a marine prodelta-delta front depositional environment for the Mid-Paleozoic red beds. A thin (9 m) black mudstone facies in the middle of the Bumita Quarry sequence might represent the Latest Devonian Hangenberg Anoxic Event. The occurrence of a Mid-Paleozoic orogeny is denied. The major regression just after the global Hangenberg Event transgressive episode is suggested as the cause of the major, pre-Carboniferous paraconformity observed in mid-Paleozoic successions of the Sibumasu/Shan-Thai Terrane.

2.4.4 Petrophysical study

Koesoemadinata and Mcmechan (2003) founds the empirical relation between measured petrophysical, SRT and ERT properties of sandstone and carbonate samples by least-squares fitting at room pressure and ambient saturation. The parameters measured were porosity, fluid permeability, clay content, grain density, bulk density, P-wave velocity, electrical conductivity and dielectric constant. The rock samples were taken from reservoir analog sites in the Ferron Sandstone in central Utah and the Ellenburger carbonate in central Texas. The relationship for